



# Graphene thin film microextraction and nanoparticle enhancement for fast LIBS metal trace analysis in liquids

F. Poggialini<sup>a,b</sup>, B. Campanella<sup>a</sup>, V. Palleschi<sup>a</sup>, M. Hidalgo<sup>c,\*</sup>, S. Legnaioli<sup>a</sup>

<sup>a</sup> Applied and Laser Spectroscopy Laboratory, Institute of Chemistry of Organometallic Compounds, Research Area of CNR, Via Giuseppe Moruzzi, 1, 56124 Pisa, Italy

<sup>b</sup> Scuola Normale Superiore, Piazza dei Cavalieri, 7, 56126 Pisa, Italy

<sup>c</sup> Department of Analytical Chemistry and Food Sciences and University Materials Institute, University of Alicante, E-03690 Alicante, Spain

## ARTICLE INFO

### Keywords:

Thin film microextraction  
Nanoparticle enhanced LIBS  
Graphene  
Signal enhancement  
Pulsed laser ablation in liquids

## ABSTRACT

Several strategies have been effectively tested in the past to improve the Laser Induced Breakdown Spectroscopy (LIBS) signal for the analysis of liquid samples, involving peculiar experimental configurations, such as Double Pulse LIBS (DP-LIBS). Recently, sample treatment has proven to be a viable and simple way to enhance the performances of LIBS towards the analysis of solutions. Among the various strategies, the most promising and versatile appears to be Thin Film Microextraction (TFME) using carbon-based adsorbents.

Another sample pre-treatment procedure, Nanoparticle-Enhanced LIBS (NELIBS), has gained significant interest due to its relative simplicity and effectiveness. This methodology uses a deposition of silver nanoparticles (AgNPs) on the sample to greatly increase the emission of the LIBS plasma.

In this work, we investigate for the first time the possibility of combining TFME and NELIBS. We developed TFME supports by depositing an aqueous graphene nano-sheets (aq-GRA) prepared by Pulsed Laser Ablation in Liquid (PLAL) on a glass substrate. The preparation of the supports was optimized with regards to the substrate nature, deposition method, sorbent volume and drying method. Then, the TFME supports were tested for the extraction of Chromium from aqueous solution at different extraction times and analyte concentration. Subsequently, the TFME supports were treated with a deposition of silver nanoparticles (AgNP) to test the feasibility of the NELIBS approach.

We observed an enhancement in the emission lines of Cr when the AgNPs were applied, as well as a lower estimated LOD value when compared to plain graphene TFME supports.

## 1. Introduction

One of the main challenges of nowadays chemical analysis is designing new analytical systems and procedures able to act as early warning analytical devices, with the aim to provide, in situ and in (almost) real-time, chemical information useful for hazard identification and forecasting of a very broad list of issues of environmental and socioeconomic concern (e.g., pollution threat warning to air or water quality, industrial process monitoring, food safety surveillance, etc.). To achieve these ambitious objectives, analytical systems should be portable, automatic and able to provide fast analytical information with the required quality for the specific use (fitness for purpose).

Conventional analytical techniques, such as Flame Atomic Absorption (FAAS), Inductively Coupled Plasma Optical Emission (ICP-OES) or Mass (ICP-MS) spectroscopies, are standard techniques able to provide

high quality analytical information. However, analytical procedures based on such conventional instrumental techniques can hardly be miniaturized, and therefore are not suitable for the task of in-situ analysis being limited to the analytical laboratory. As a consequence, the trend of today's analytical chemistry is shifting towards the development of small-size and fully automated instrumentation useful for field operation, able to promptly provide essential information about potential risks which can be further corroborated by the more sensitive, but also more expensive and bulky, laboratory instruments.

Laser Induced Breakdown Spectroscopy (LIBS) has many characteristics that make it one of the ideal candidates for an early warning system. LIBS is able to analyze almost any kind of sample directly, in a wide range of ambient conditions. The instrumentation can also be scaled down to be sufficiently portable, and robust enough for remote or in-situ measurements. For these reasons, many applications of LIBS can be

\* Corresponding author.

E-mail address: [montserrat.hidalgo@ua.es](mailto:montserrat.hidalgo@ua.es) (M. Hidalgo).

<https://doi.org/10.1016/j.sab.2022.106471>

Received 10 March 2022; Received in revised form 6 June 2022; Accepted 7 June 2022

Available online 10 June 2022

0584-8547/© 2022 The Authors. Published by Elsevier B.V. This is an open access article under the CC BY-NC-ND license (<http://creativecommons.org/licenses/by-nc-nd/4.0/>).

found in the monitoring of industrial processes, quality control of pharmaceutical and food production, but also in the archeology and cultural heritage fields as well as in space exploration [1,2].

Nevertheless, one of the major drawbacks of LIBS is the low performance for the analysis of liquid samples, as LODs that can be reached with LIBS are in the order of tens or hundreds of mg/L. When compared to conventional analytical techniques such as Flame Atomic Absorption (FAAS), Inductively Coupled Plasma Optical Emission (ICP-OES) or Mass (ICP-MS) spectroscopies, the LODs that can be reached with LIBS are much higher, in the order of tens or hundreds of mg/L. Over the years, several methods have been proposed to enhance the performance of the technique for the analysis of liquid samples, either by improving the instrumental setup or by treating the analyzed samples [3] [4]. For example, some works propose to perform the LIBS measurement directly on the surface of the liquid sample, to generate an aerosol or a liquid jet to increase the performance of the technique [2]. On the other hand, some authors propose to convert the liquid matrix into a solid in order to eliminate many of the issues [5–8].

Surface Enhanced LIBS (SENLIBS) can also be used for improving the capabilities of LIBS in the analysis of liquid samples. This approach consists in the deposition and drying of a liquid sample on a suitable substrate (i.e. a conductive material like a metal sheet or a semiconductor like a silicon wafer), onto which the LIBS measurement is performed. The conductive nature of the substrate can greatly aid in the generation of the laser plasma, as well as to increase the plasma temperature and emission from the analyte species.

Aras and co-workers [5] investigated a method for the detection of ultra-trace of heavy metals in aqueous droplets using LIBS. In their work, they coupled the enhancing effects of SENLIBS, using Ni, Mn-alloy, Zn and Si substrates, with a liquid-liquid extraction to pre-concentrate the analytes before drying sample droplets onto the substrates. This allowed the authors to obtain LODs of tens of pg/ $\mu$ L for Cd, Pb and Cu. Similarly, Niu et al. [6] investigated the use of laser pre-treated aluminum substrates for the SENLIBS detection of heavy metals in aqueous solutions. The authors found that the rough microstructure on the substrate surface trapped the solution in the laser-pretreated area and enabled a homogeneous distribution of the solution, enabling LODs of tens of  $\mu$ g/L for Cd and Cr. Ma and co-workers investigated SENLIBS for the detection of heavy metals in aqueous solutions using Zn, Mg alloy, Ni and Si substrates [9]. After drying droplets of stock solutions onto the substrates, the authors obtained LODs of less than 0.004 mg/L of Pb and Cr. Similarly, Aguirre et al. demonstrated that SENLIBS can greatly improve the sensitivity of LIBS towards the analysis of liquid samples, compared to the direct analysis of microdroplets [10]. In their work, the authors used LIBS to analyze liquid samples dried onto an aluminum and obtained a LOD of 6  $\mu$ g g<sup>-1</sup> for Mn, against a LOD of 0.2% for the direct analysis of the liquid droplets. Nevertheless, SENLIBS does not allow for the pre-concentration of analytes, as the sample solution is deposited on the substrate as-is. This could hinder the detection of analytes when their concentration is too low to obtain a homogeneous deposition on the SENLIBS substrate (e.g. drying multiple droplets on the same spot can produce coffee ring effects).

An alternative route to improve the LODs for metals in solution is the use of Solid Phase Extraction (SPE) techniques and, in particular, of Solid Phase Microextraction (SPME). SPME uses a small amount of a sorbent material (a few  $\mu$ g) to extract and concentrate the analytes in a solution and therefore minimizes the amount of sorbent needed, while allowing for very fast extraction times.

Wang et al. [11] were the first to combine SPME and LIBS for the determination of metals in aqueous solutions. In their work, they used a Dispersive SPME (D-SPME) methodology based on graphite nanoparticles, combined with a preemptive chelation of the metals in solution. The analysis of the dried solid phase allowed for the determination of Cr, Mn and Ag at concentrations of 17  $\mu$ g/L and lower. Subsequently, Ruiz et al. [12] proposed an improvement of the D-SPME method by using Graphene Oxide (GO) as an adsorbent. They were able to eliminate

the metal chelation step during sample preparation and still obtain LODs lower than 50  $\mu$ g/L.

While D-SPME can be relatively easy to couple with LIBS, there is still the issue of recovering the extractant from the liquid sample, drying it and treating it to produce a suitable matrix for LIBS, which makes this microextraction procedure difficult to automate. This drawback can be surmounted with the use of Thin Film Microextraction (TFME) modality. TFME uses a solid substrate coated with a thin layer of sorbent material. This allows for an easier recovery of the sorbent phase as it remains adhered to the rigid substrate during the extraction, and the analyte-enriched sorbent is ready to be analyzed by LIBS without the need of additional treatments. While a desorption phase is generally required for analysis with conventional techniques, this step is not necessary if LIBS is used for the measurement. Ripoll et al. [13] demonstrated the effectiveness of a combined TFME-LIBS approach for the extraction of heavy metals from aqueous solution. Using GO as an adsorbent, the authors prepared TFME supports by mould deposition and obtained LODs in the order of 50  $\mu$ g/L. Recently, Ripoll and co-workers also investigated an improved methodology for the preparation of TFME supports, based on electrospray deposition (ESD) of GO [14]. In this work the authors obtained even lower LODs, in the order of 15  $\mu$ g/L, demonstrating the increased performance of the ESD supports over other deposition methods.

Another methodology proposed to enhance LIBS performance is Nanoparticle Enhanced LIBS (NELIBS), proposed by De Giacomo et al. [15]. This methodology is of particular interest for its fast and relatively easy implementation. In brief, the technique allows for the improvement of the LIBS technique capabilities and analytical response by using a dispersion of noble metal nanoparticles (NPs) deposited on the sample surface, and a subsequent LIBS analysis performed on such deposition. The interaction of the laser electromagnetic field with the surface conduction electrons of the NPs induces a polarization and strong oscillation of the electrons (Localized Surface Plasmon, LSP) and, in turn, a charge accumulation on the NPs borders. The generated dipole produces a large electromagnetic enhancement confined to the NPs surface and the adjacent regions. This phenomenon effectively increases the intensity of the electromagnetic field induced by the laser on the sample surface, the number of emitted electrons, the ablated mass and the plasma emission intensity. The authors have reported enhancement in the intensity of the LIBS signal in optimal conditions of up to two orders of magnitude. A recently published review by Dell'Aglio et al. [16] thoroughly describes the phenomena and the mechanisms correlated to NELIBS, while highlighting the criticalities of the approach. NELIBS was successfully used to enhance the performances of LIBS towards the detection of metals in liquids by depositing droplets of the analyte solution on a layer of dried NPs, in a similar fashion to the SENLIBS approach [17].

In a work by Wen et al., a substrate prepared using AuNPs and porous electrospun ultrafine fibers was tested successfully for the detection of  $\mu$ g/mL heavy metals in aqueous samples [18]. The authors showed how the structure of such substrate, coupled with the AuNPs can greatly improve the detection of the extracted analytes, thanks to the large surface area of the fibers. Nevertheless, the preparation of the fibers requires a dedicated instrumentation and knowledge on how to operate it to obtain an optimal product. For comparison, a work by Pramanik et al. [19] proposes a methodology for the preparation of an aqueous dispersion of graphene nano-sheets from graphite using a pulsed laser.

In this work we discuss the feasibility of a combined approach of TFME and NELIBS. To the best of our knowledge, this is the first time such an approach has ever been proposed and tested for the determination and LOD estimation of heavy metals extracted from aqueous solutions. Moreover, both the AgNPs and the graphene were prepared using the same PLAL setup, significantly reducing complexity, costs and the time required for the experiments.

## 2. Materials and methods

### 2.1. Materials and AgNP preparation

Aqueous dispersions of graphene nano-sheets (aq-GRA) were prepared starting from pure graphite (Graphite flakes, Sigma-Aldrich).

Glass microscope slides (Plain microscope slides, J. Melvin Freed Brand, USA) were cut to approximately  $1 \times 1.5$  cm pieces and used as substrates for the preparation of TFME supports. Chemical etching of the glass slides was performed using a commercially available glass etching paste (Idea VETRO etching paste, Maimeri, Italy).

Silver nanoparticles (AgNPs) were prepared by Pulsed Laser Ablation in Liquid (PLAL). Silver foil (2 mm thickness, 99.9% trace metal basis from Sigma-Aldrich) and a 2 mM KCl (powder, Sigma-Aldrich) aqueous solution were used for PLAL synthesis of AgNPs. The procedure for the preparation of AgNPs is described in detail in a recent work by Botto et al. [20]. In brief, a pulsed laser, operating at the fundamental wavelength of 1064 nm, with a repetition rate of 10 Hz and a pulse energy of 100 mJ, was focused on a silver target immersed in the KCl solution. After an ablation time of 5 min, the AgNPs dispersion was characterized by UV–Vis spectroscopy (Jasco V-750 double beam spectrophotometer, scans from 300 nm to 600 nm, scan rate 300 nm/min). The values of maximum absorbance at the corresponding wavelength in the spectrum can be used to readily estimate the size and concentration of the NPs solution using Lambert-Beer's law and the data indicated in literature [21]. The synthesized nanoparticles were found to have an average diameter of 11 nm and a mass concentration of 0.02 mg/mL ( $[NP] \approx 4.6$  nM).

Standard aqueous solutions containing  $Cr^{3+}$  were prepared by appropriate dilution of 1000 mg/L mono-element stock solutions (High-Purity mono-element standard solutions, Charleston, UK). Deionized water was obtained from an Elga Purelab Option DV 35 (Veolia Environment, France) water filtration system, and used throughout the study.

### 2.2. aq-GRA preparation

The procedure for the preparation of the aq-GRA was adapted from the work of Pramanik et al. [19].

A dispersion of graphite flakes was prepared, having a concentration of 10 mg/mL, using Milli-Q water. The dispersion was sonicated until the graphite was fully dispersed ( $2 \times 30$  min sessions). 2 mL of this dispersion were placed in a clear glass vial sealed with plastic screw-caps for headspace analysis. The vial was placed sideways under the path of the laser beam.

The laser was operated in repetition mode with a shot frequency of 10 Hz, while the pulse was focused inside the liquid. The irradiation time was 5 min and the shock from each laser pulse was sufficient for stirring the dispersion inside the vial. After the irradiation, the vial was removed and allowed to cool down. Built up pressure was vented by inserting a syringe needle into the vial through the cap septum. The irradiation process was repeated three times, for a cumulative irradiation time of 15 min. The dispersion was then sonicated for 30 min ( $2 \times 15$  min sessions with 5 min of cooling time in between) at room temperature.

At the end of the preparation procedure, a homogeneous black dispersion was obtained, with no discernible flakes at the naked eye. The dispersions were deposited on a glass slide and analyzed using a Renishaw RM 2000 Raman instrument, coupled with an optical Leica DLML microscope, equipped with a  $50\times$  NPLAN objective. The laser source was a He–Ne laser with a wavelength of 633 nm and a laser power output on the sample of about 0.07 mW. Several spectra were registered on different depositions, obtaining perfectly reproducible results. The spectra were compared to those reported in literature [19,22,23] (Fig. 1).

The Raman spectra show the presence of strong G ( $\approx 1580$   $cm^{-1}$ ) and 2D ( $\approx 2685$   $cm^{-1}$ ) bands. The relatively broad, but symmetrical, 2D

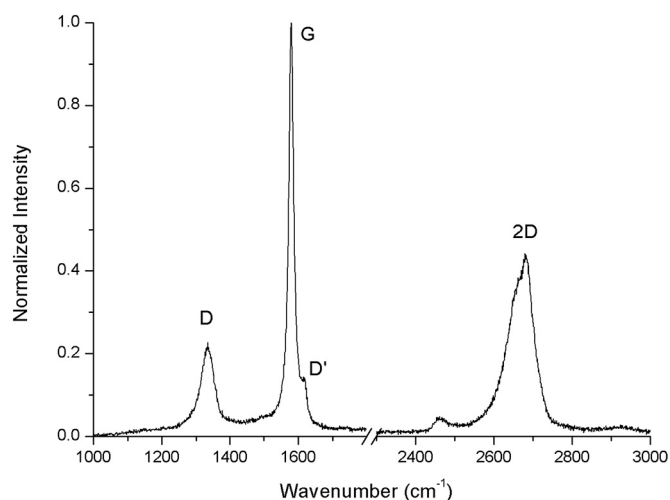


Fig. 1. Normalized Raman spectrum of the prepared aq-GRA deposition.

band confirms the presence of a multilayer structure of graphene, coherent with the deposition methods. Moreover, the presence of the D' ( $\approx 1615$   $cm^{-1}$ ) and the D ( $\approx 1350$   $cm^{-1}$ ) bands, suggests the introduction of defects in the graphene structure during the PLAL process, such as oxygen- and hydroxyl-containing groups. This is not unwelcome for this work, as it can increase the extraction power of the aq-GRA similarly to the behavior observed in the case of graphene oxide [24,25].

Graphite oxide and graphene oxide can be characterized by an ambivalent hydrophobic/hydrophilic nature, allowing the adsorption of both organic compounds and metal ions. Due to the presence of oxygen-containing functionalities (in form of epoxy, hydroxyl and carboxyl groups) on the material surface, successful removal of metal ions from aqueous solutions is possible without the need of any previous metal complexation step, since these functional groups have lone electron pairs that can be shared for binding metal ions forming metal complexes which, along with electrostatic attraction and ion exchange, are the mechanisms responsible for metals ion adsorption. This fact represents an important advantage over other extensively used adsorbents such as activated carbon, for instance, which needs a previous metal chelation step in order to improve its adsorption capacity for metal ions [12,26]. In any case, it should be noted that the pH of the sample solution affects the surface chemistry of the graphite oxide and related products due to ionization equilibrium of the different oxygen-containing functional groups. Low pH values lead to a positively charged graphene oxide surface because of protonation of the functional groups, whereas high pH values induce negatively charged surface due to deprotonation. The pH at which the surface charge of the adsorbent is zero is denoted as point of zero charge ( $pH_{pzc}$ ). This implies that pH values above the  $pH_{pzc}$  of the material will lead to a negatively charged surface, resulting in conditions that are more favorable for interaction with positively charged metal ions [27,28]. Besides its influence on the adsorbent surface chemistry, pH also affects the proportion of the various metal ion species present in solution due to hydrolysis (e.g.,  $M^{2+}$ ,  $M(OH)^+$ ,  $M(OH)_2$ ,  $M(OH)_3^-$ , ...). At low pH values but still above the  $pH_{pzc}$  of the adsorbent material, the relative proportion of  $M^{n+}$  and positively charged M species is high, and metal ions adsorption can occur through several mechanisms, such as electrostatic attraction, ion exchange and/or surface complexation. At the other extreme (i.e., highly alkaline conditions) the proportion of negatively charged metal species in solution increases (e.g.,  $M(OH)_3^-$ ,  $M(OH)_4^{2-}$ ) and, due to electrostatic repulsion, these species are hardly adsorbed on the negatively charged binding sites of the adsorbent [26,29]. As such, it is evident how pH conditions can affect the overall extraction of metal ions by graphite or graphene oxide.

$pH_{pzc}$  of graphite and related materials is well-known to be below 4

[30], and formation of negatively charged species of the target metals, or precipitation of the metal hydroxides, occurs at pH values above 7 [31,32]. In base to these bibliographic data, a solution pH of 7 was used throughout the experimental work in this feasibility study.

### 2.3. Instrumentation

This work was performed using the LIBS instrumentations provided by the ICCOM-CNR in Pisa (Italy) and the University of Alicante (Spain). The former was used during the aq-GRA and AgNPs preparation as well as the investigation of the optimal parameters for support preparation, extraction and NELIBS, while the latter was used for building calibration curves and for NELIBS experiments.

At CNR, LIBS analyses were performed using the Modì portable LIBS instrument [33]. Modì is equipped with a Nd:YAG laser (LS2134-D, Lotis Lasers) operating at the fundamental wavelength (1064 nm) and delivering two laser pulses of up to 110 mJ per pulse in 15 ns FWHM. In this work, the system was operated in single-pulse mode. The maximum pulse repetition rate is 10 Hz. The laser beam is focused into an experimental chamber and the plasma emission is collected by an optical fiber placed at a distance of 1 cm from the sample and at an angle of 45° with respect to the laser beam. The ablation spot is about 300 μm. The system was coupled with an Aryelle 200 Echelle spectrograph (200 nm to 790 nm, LTB Lasertechnik Berlin) coupled with an air-cooled ICCD (iStar DH334T-18F03, Andor), with a resolving power of 9000. The acquisition delay was set to 500 ns after the second laser pulse and the integration time was 10 μs, in accordance with routine LIBS analyses. The spectrometer was calibrated with a Deuterium-Halogen lamp (Ocean Optics DH-2000).

At the University of Alicante, the LIBS instrument used a Nd:YAG laser (Handy-YAG model HYL 101, Q-switched, Quanta System S.P.A., Varese, Italy), operating at the fundamental wavelength with a nominal pulse width of 6 ns FWHM, and a compact time-integrated spectrometer (five channel spectrometer, model AvaSpec-2048-SPU, Avantes, Eerbeek, The Netherlands). The laser is focused on the sample by a 60 mm focal length biconvex lens. The sample is placed on a manually-operated x/y translation stage. Plasma emission is collected and sent to the entrance slit of the five-channel spectrometer by a five-furcated optical fiber (5 × 400 μm fiber optic cable, model FC5-UV400-2, Avantes, Eerbeek, Netherlands), which is positioned at 60° with respect to the incident laser beam and at approximately 2 cm from the sample surface. The ablation spot was estimated at approximately 170 μm. Each measurement is externally controlled by manually triggering the laser firing sequence (i.e. external triggers are sent to the laser flash-lamp and Q-switch) with two pulse generators (Digital delay/pulse generator, model DG 535, Stanford Research Systems, Inc. and 1 MHz–50 MHz pulse/function generator, model 8116A, Hewlett Packard/Agilent Technologies, Santa Clara, USA). The laser pulse and the spectrometer are further synchronized with the aid of the spectrometer software (AvaSoft©, v8.5.0.0, Avantes, Eerbeek, Netherlands). Each laser pulse had an energy of approximately 180 mJ. LIBS spectra were collected 1.5 μs after the plasma generation, with a 1 ms integration time (set by the manufacturer).

All the LIBS spectra were analyzed using the in-house developed LIBS++ software.

The PLAL setup was the same for the preparation of both the aq-GRA and NPs. The system uses a double pulse Nd:YAG laser (LS-2134D, Lotis) operating at the fundamental wavelength of 1064 nm. The laser was operated in single pulse mode, with a pulse energy around 130 mJ in 25 ns.

### 2.4. Glass substrates and TFME supports optimization

The method chosen for the preparation of the TFME supports was the drop casting of the aq-GRA on the glass substrates, followed by thermal drying. Other methods of preparation were considered, but ultimately

discarded for this work. Dip coating using a home-built apparatus and electrospray deposition showed that the time required for the preparation of the number of substrates required for this study was too inefficient, with the added disadvantage of a much higher complexity of the preparation procedure and instrumentation of electrospray technique. Additionally, spin coating was not employed due to the high volumes of aq-GRA required for a homogeneous coating of the substrates.

Untreated microscope glass slides (suitably cut) were tested alongside mechanically and chemically etched slides. Mechanical etching was performed using a high-speed rotary tool with an abrasive tip. One face of each substrate was grinded as homogeneously as possible, then washed thoroughly with tap water, deionized water and dried on a hot plate. Chemical etching was conducted by following the specifications of the manufacturer of the etching paste. In brief, the paste was applied to one side of the glass slides and left to react for 15–20 min. Once the etching reaction occurred, the slides were cut to the required dimension, washed and dried.

An example of the etched glasses is reported in Fig. 2.

To identify the optimal procedure for drying the aq-GRA onto the glass substrates, various methods were tested on both the mechanically and chemically etched substrates. Plain glass slides were used as a benchmark by drop casting 10 μL of aq-GRA on their surface.

Drying the supports in open air at room temperature was not considered as the time required was in the order of several hours. Drying using a flow of hot air (using a heat gun or a blow dryer) was tested with some success, reducing the drying time significantly (from hours to tens of seconds). However, it was noticed that the droplets were not drying homogeneously, showing visible “coffee rings” and halos. Moreover, the air flow caused some droplets to deform and occasionally spill out of the substrates.

More promising results were observed while drying the supports on a hot plate. The temperature was set around 90 °C to avoid boiling of the liquid. When the supports were placed in direct contact with the plate, however, it was noticed that the drying process was often not homogeneous, and the graphene layer cracked and failed to adhere properly to the glass. This was remedied by placing a double layer of paper towel between the substrates and the hot plate surface. This had the effect of slightly slowing down the drying process, making it more homogeneous and less violent. The result was a nearly perfect circular layer of graphene deposited on the glass surface.

This procedure was followed by preparation of TFME supports with plain and etched glass slides using in all cases 10 μL of aq-GRA, and the results are reported in Fig. 3. A deposition of 10 μL of graphite on plain glass was added for a visual comparison.

As it can be seen, the best results are obtained using plain glass and chemically etched glass. When the aq-GRA is deposited on mechanically etched glass substrates, the droplets do not conserve their shape and tend to dry in a disordered fashion, which can severely hinder the reproducibility of the extraction procedure and LIBS measurement.

To test the stability of the different supports against immersion in a liquid, three TFME supports of each type were inserted in a plastic vial containing 1.5 mL of H<sub>2</sub>O. It was rapidly observed how the plain glass supports are extremely fragile and unsuitable for TFME, as the graphene layer detached immediately on contact with the water, remaining afloat on the surface (while maintaining the circular structure). The mechanically etched supports showed a higher tolerance to immersion and manipulation. Nevertheless, this etching procedure cannot produce homogeneous and reproducible patterns, and some supports crumbled and broke off the glass shortly after immersion or upon removal from the vial. The best results were obtained with chemically etched supports. As well as being the most homogeneous, they showed a surprisingly high resilience to manipulation and immersion, remaining intact even after 24 h of continued immersion.

As a result, the TFME supports used throughout the study were prepared using chemically etched glass substrates, with drop casting of aq-GRA, and dried on a hot plate with paper towel partial insulation.



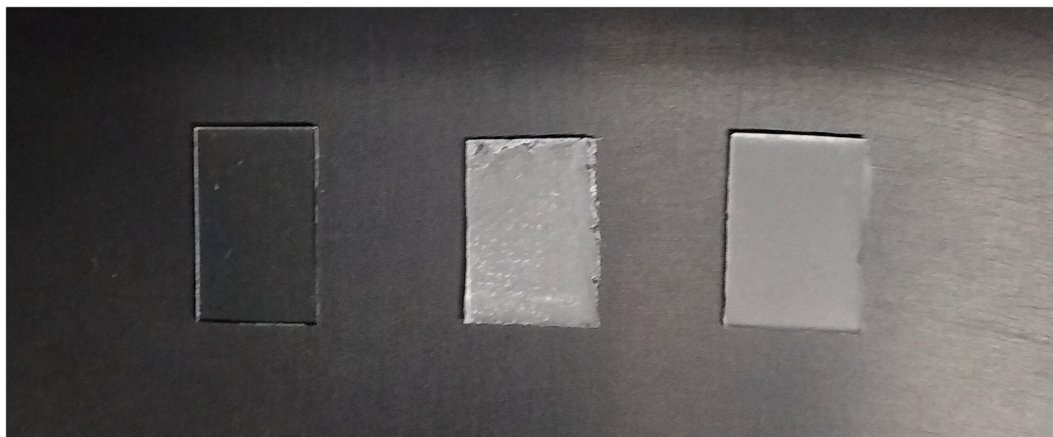


Fig. 2. Different types of glass substrates. Plain glass (left), mechanically etched (center) and chemically etched (right).

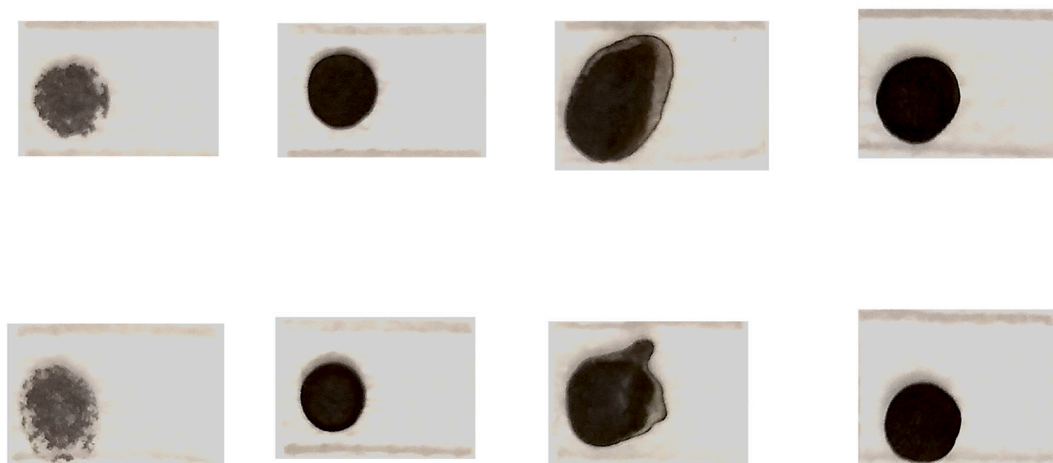


Fig. 3. TFME supports prepared with different glass substrates. From left to right: graphite on plain glass, graphene on plain glass, graphene on mechanically etched glass, graphene on chemically etched glass.

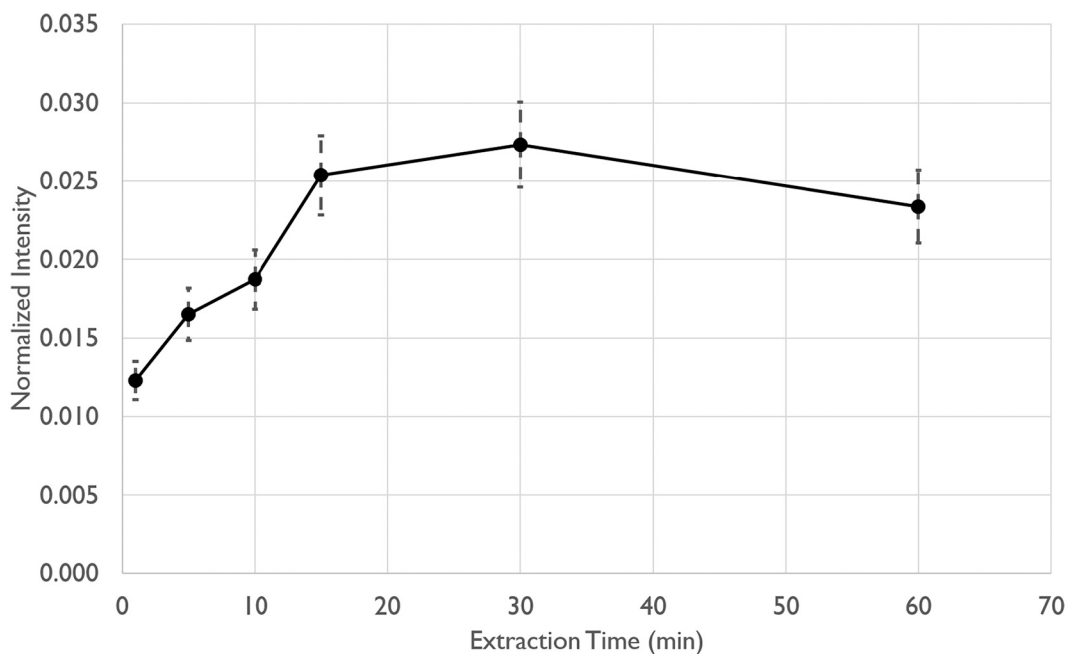


Fig. 4. Normalized intensity of Cr I (360.5 nm) depending on the extraction time. Reported errors are derived from LIBS uncertainty.

### 3. Results and discussion

#### 3.1. TFME conditions optimization

To determine the optimal extraction procedure, supports were prepared using 10  $\mu\text{L}$  of aq-GRA. The supports were then immersed on aqueous solutions containing 20 mg/L of Cr (pH  $\approx$  7) for an increasing amount of time, namely 5, 10, 15, 30 and 60 min. After the extraction process, each support was removed from the solution and dried on a hot plate with paper towel insulation for approximately 15 min, to ensure complete evaporation of the liquid. Each extraction test was repeated three times and the obtained LIBS spectra were averaged. The results are reported in Fig. 4.

Y-axis in Fig. 4 represents the integrated intensity of Cr I emission line at 360.5 nm, normalized on the total integrated intensity of each spectrum.

It can be observed how there is a pronounced growth of the Cr intensity in the first few minutes of the extraction process. After 15 min of immersion, the signal appears to stabilize, with a shallow decline towards 60 min of immersion. This can be ascribed to both the saturation of the free sites on the support, where the metal ions can be adsorbed, as well as to the microscopic degradation of the graphene layer due to the prolonged exposure to the aqueous environment.

For this study, an extraction time of 15 min was considered optimal, as it guaranteed a high signal from the analyte, while keeping the extraction time relatively short. The small increase in signal intensity at 30 min of extraction was not deemed strong enough to justify doubling the extraction time.

To find the optimal volume of aq-GRA for the preparation of the supports, various drop castings were realized, increasing the deposited volume of aq-GRA in 10  $\mu\text{L}$  aliquots. Indeed, low sorbent volumes can hinder the extraction of the analytes from the samples and lead to quick saturation of the supports. Additionally, if the graphene layer is too thin, an ablation of the underlying glass during LIBS could be observed, and this may give rise to interferences. Generally, a higher volume of adsorbent is always preferable, as it increases the number of binding

sites for the analytes, as well as increasing the efficiency of the extraction [34]. In this work, however, it was quickly observed that preparing supports with large amounts of aq-GRA was not feasible. 20  $\mu\text{L}$  depositions ( $2 \times 10$   $\mu\text{L}$  aliquots) allowed for the preparation of homogeneous and robust supports, which easily handled the extraction and subsequent manipulations. Increasing the deposition volume to 30  $\mu\text{L}$  ( $3 \times 10$   $\mu\text{L}$  aliquots) caused the formation of disordered flakes and non-homogeneous layers of graphene. Such layers had the tendency of breaking off during the extraction or cracking during the drying process, hindering the LIBS measurement greatly. It was then decided to limit the aq-GRA volume to 20  $\mu\text{L}$  for this study. The thickness of the deposited graphene layer was estimated at approximately 40  $\mu\text{m}$  by preparing a cross section of a TFME support and observing it under an optical microscope (Leica DLML, 50 $\times$  magnification).

New TFME supports were used for building calibration curves from the extraction of Cr in aqueous solutions. Five standard solutions with Cr concentration in the range 0.05 mg/L – 1 mg/L were prepared by dilution of a 1000 mg/L chromium stock solution. The extraction procedure was repeated five times for each concentration and the resulting spectra were averaged. The results are shown in Fig. 5.

By fitting the experimental data with a polynomial curve, it can be observed how the signal intensity sharply grows for the first three concentration values and then the growth flattens to a plateau for higher concentrations, which reduces the dynamic range of this method for Cr analysis. This can be ascribed to the relatively low volume of aq-GRA that is used to produce the supports. The free sites are rapidly and readily occupied by the metal ions and higher concentrations can saturate the supports during the extraction time. In fact, a similar trend was observed in previous experiments using higher concentrations of Cr (not shown in this work), and the plateau was observed around the same value of concentrations reported here.

If the two points relative to the higher concentrations are removed (i. e. 1 mg/L and 0.5 mg/L), the calibration curve becomes linear and reaches a value of  $R^2 = 0.9971$ . The LOD for Cr was estimated from the linear part of the calibration curve using the IUPAC formula  $LOD = \frac{3\sigma}{Slope}$  and it was found to be 0.055 mg/L.

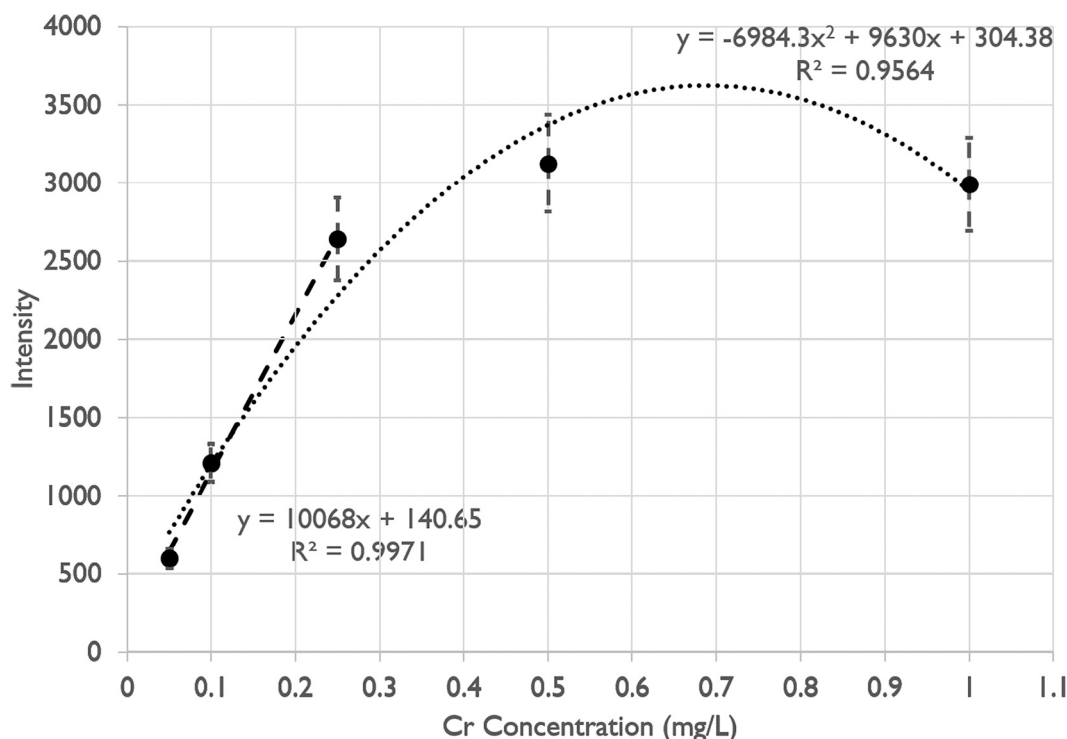


Fig. 5. Calibration curves for Cr using graphene supports. Reported errors are derived from LIBS uncertainty.

### 3.2. NELIBS and TFME coupling

To investigate the possibility of combining the NELIBS approach with the obtained TFME supports, three different methods for the integration of the AgNPs with the graphene layer were tested.

The first method (Top Deposition, TD) follows the typical procedure of NELIBS, with a deposition of 10  $\mu\text{L}$  AgNP dispersion on top of the graphene support after the extraction procedure, which is then dried.

In the second method (Bottom Deposition, BD) 10  $\mu\text{L}$  of AgNPs were deposited on a chemically etched glass substrate, dried and the aq-GRA was deposited on top of the nanoparticles. This approach is similar to the SENLIBS technique, described in the work of De Giacomo et al. [17].

The last method (Composite, C) that was investigated was the preparation of a composite dispersion of AgNPs and aq-GRA. To prepare the composite a given volume of aq-GRA dispersion was centrifuged to separate the graphene from the solvent, which was removed. The graphene was then dispersed in the same volume of the AgNPs solution, sonicated and then used to prepare the TFME supports by using, as in the previous methods, 10  $\mu\text{L}$  of GRA-AgNPs dispersion. The method was tested using various AgNPs concentrations. The results reported in this work refer to the supports that gave the best results, which corresponded to an AgNPs concentration of 0.02 mg/mL.

Each type of support was used for the extraction of a 0.2 mg/L Cr solution and the Cr I (360.5 nm) emission line was monitored. The tests were repeated five times and the resulting spectra were averaged. The Enhancement Factor (EF) for NELIBS was obtained as the ratio of the emission intensity of the Cr line between plain graphene supports and the various AgNPs treated supports. The results are reported in Fig. 6.

As reported in Fig. 6, the EF values for both BD and C supports are close to 1, meaning that almost no discernible signal enhancement was observed. In the case of BD, this can be attributed to the complete absorption of the laser pulse by the graphene layer. This effectively prevents the interaction of the laser with the underlying AgNPs, rendering them ineffective. On the other hand, the presence of AgNPs in direct contact with the graphene during the preparation of the C supports can contribute to a partial saturation of the free sites in the graphene by the adsorption of the metal nanoparticles, which would then hinder the extraction of the analytes from the sample solutions.

The highest observed values for EF were obtained for the conventional NELIBS sample preparation method, that is the deposition of AgNPs directly on the graphene. As such, this method was chosen for the subsequent experiments.

To determine the optimal amount of AgNPs that should be used on the graphene supports, various tests were conducted while increasing the aliquot of AgNPs (in 10  $\mu\text{L}$  increments) deposited. Each test was repeated five times and the resulting spectra were averaged. A 0.2 mg/L Cr solution was used for the extraction and the Cr I (360.5 nm) emission

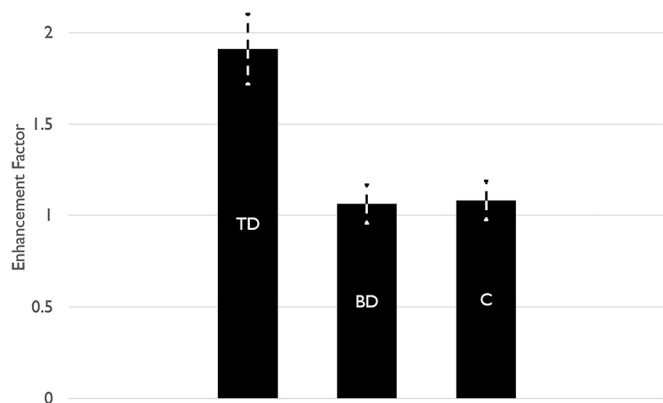


Fig. 6. Signal enhancement for different TFME support types. Reported errors are derived from LIBS uncertainty.

line was monitored. In Fig. 7 are reported the observed values of EF.

The highest EF values observed were obtained for an AgNPs deposition of 20  $\mu\text{L}$  ( $2 \times 10 \mu\text{L}$ ) on the graphene supports. It should be noted that 30  $\mu\text{L}$  ( $3 \times 10 \mu\text{L}$ ) was chosen as the upper limit because adding more AgNPs to the graphene supports severely compromised their integrity, causing cracks and breaking up the layers.

Using the experimental parameters obtained in the previous tests, the graphene supports combined with a AgNPs deposition were used to build a calibration curve for Cr. Five Cr standard solutions in the concentration range 0.05 mg/L – 1 mg/L were prepared. The extraction procedure was repeated five times for each concentration and the resulting spectra were averaged. The results are shown in Fig. 8.

It can be seen that the calibration curve for nanoparticle/graphene supports (NPGRA) has a similar trend to that of plain graphene, reaching a plateau between 0.3 and 0.5 mg/L of Cr.

By removing the two points relative to the higher Cr concentrations, as it was done for the graphene curve, a linear calibration curve can be obtained with a value of  $R^2 = 0.9905$ . The increase in signal enhancement due to the application of the AgNPs also allows for a slightly lower LOD than the one obtained from the graphene calibration. The NPGRA LOD was estimated to be 0.032 mg/L.

A summary of the data obtained is reported in Table 1.

By observing the values of  $R^2$  and the LODs obtained from the linearized calibration curves, it can be deduced that adding the AgNPs to the graphene supports does not improve the quality of the fitted curve. Indeed, the values of  $R^2$  remain quite similar. Nevertheless, a decrease in the LOD for Cr of about 40% is registered when using the AgNP/GRA TFME supports. This result is encouraging, and hints strongly to a potential use of the NELIBS effect for the improvement of the performances of TFME supports for LIBS analysis with a minimal increase in the complexity of the sample preparation procedure, as well as in the costs and time required for the analysis when compared to conventional TFME approaches. Indeed, further optimization of the experimental procedure and of the TFME supports would surely result in even better LODs and dynamic ranges for the proposed technique.

### 4. Conclusions

A novel approach to the NELIBS technique for the signal enhancement of LIBS was proposed in this work, combining the enhancing effects of AgNPs and NELIBS with the TFME methodology.

Graphene nanosheets were successfully prepared using a pulsed laser and used for the preparation of TFME supports. Various kinds of glass substrates were tested and the procedure for the preparation of the TFME supports was optimized. TFME supports prepared using 20  $\mu\text{L}$  of aq-GRA on chemically etched glass were prepared and successfully used

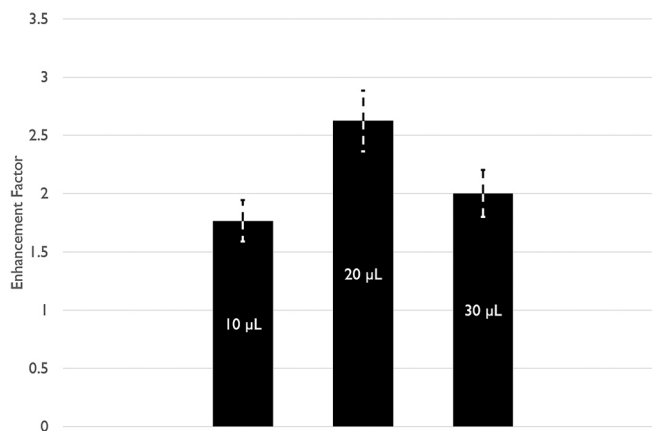


Fig. 7. Signal enhancement for different deposited volumes of AgNPs dispersion. Reported errors are derived from LIBS uncertainty.

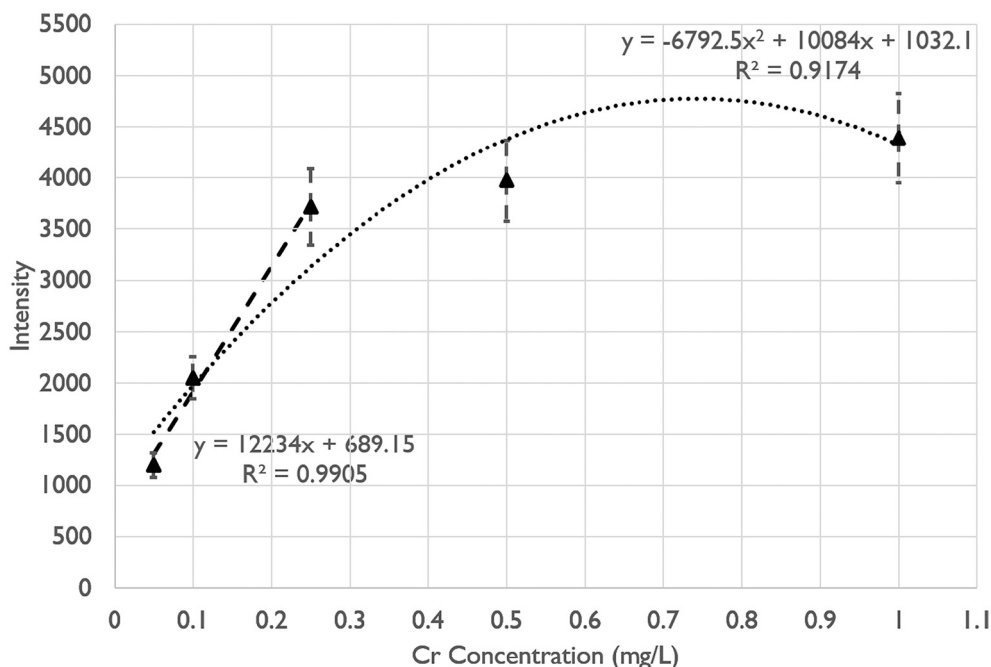


Fig. 8. Calibration curves for Cr using NPGRA supports. Reported errors are derived from LIBS uncertainty.

Table 1

Values obtained from the calibration curves for Cr in the case of graphene and NPGRA supports. n/a: value not estimated for the curve.

	R <sup>2</sup>	Cr LOD (mg/L)
Graphene Non-Linear Calibration	0.9564	n/a
Graphene Linear Calibration	0.9971	0.055
NPGRA Non-Linear Calibration	0.9174	n/a
NPGRA Linear Calibration	0.9905	0.032

to build a calibration curve for Cr, ranging from 0.05 mg/L to 1 mg/L. A LOD value was estimated at 0.055 mg/L. Subsequently, 20  $\mu$ L of AgNPs were deposited on the TFME supports after the extraction procedure, and a similar calibration curve was obtained. In this case, the LOD could be estimated at 0.032 mg/L, demonstrating that the NELIBS approach can be coupled with TFME to allow for lower LODs than the one obtainable using plain graphene. It should be noted that even if a pH of 7 was used in this work, optimization of this parameter needs to be carried out in future studies, due to the importance of this experimental factor for metal ions extraction and to the fact that the optimal pH value for different metals can vary depending on several factors (e.g., metal electronegativity, stability constant of the metal hydroxide, metal complex resulting from the interaction with the functional groups of the adsorbent surface, etc.).

Despite the encouraging results obtained in this research, further studies should be carried out to explore possible variations in the methodology, with the aim to surmount the different drawbacks identified in the current viability study. For instance, the currently observed narrow linear range of the method could be extended by investigating different deposition methods for both the graphene and the AgNPs and/or by optimizing the quantity of adsorbent deposited on the substrate, in order to increase the surface area available for adsorption. Additionally, the preparation of a ready-to-use AgNP/GRA composite would further simplify the procedure, enabling the use of this technique for in-situ and online measurements.

In addition to the results presented in this work, a batch of supports

was used to test their performance towards the extraction of a multi-elemental aqueous solution containing Cu<sup>2+</sup>, Cr<sup>3+</sup>, Ni<sup>2+</sup> and Pb<sup>2+</sup> in a concentration range of 0.01 mg/L – 0.25 mg/L. However, due to the almost complete non-specificity of graphene, the observed results were not optimal and it was observed that not all analytes followed the same trend with increasing concentration. Cu and Cr intensities grew from 0.01 mg/L to 0.1 mg/L and then reached a plateau, while the intensity of Pb appeared to remain more or less constant throughout the experiment. Additionally, it was not possible to determine the presence of Ni. While these results show that the prepared TFME supports are not suitable as-is for the analysis of multi-elemental solutions, further studies should be conducted where experimental conditions such as the pH of the solution, the presence of chelating agents or competing species are taken into consideration.

It should also be stressed out that while using larger volumes of aq-GRA for the preparation of TFME supports might help to mitigate the issues of saturation of the available sites for metal absorption, it still does not solve the universal character of graphene as a sorbent. Indeed, the use of functionalized graphene would allow for the preparation of supports that can be specifically tuned for the extraction of a single analyte. Even though this method would significantly increase the difficulty of the support preparation procedure, it should be also investigated in future studies.

## Funding

M. Hidalgo is grateful to Ministerio de Economía, Industria y Competitividad [CTQ2016-79991-R] and Conselleria de Educació, Investigació, Cultura y Deporte (Regional Government of Valencia, Spain) [PROMETEO/2018/087] for the financial support.

## Novelty statement

To the best of the authors' knowledge, it is the first time the combination of Thin Film Microextraction (TFME) with Nanoparticles-enhanced LIBS (NELIBS) detection has been proposed as a methodology able to improve the performance of LIBS for liquid samples analysis. The results are encouraging and further demonstrate the versatility of the NELIBS approach.



## CRedit authorship contribution statement

**F. Poggialini:** Conceptualization, Methodology, Investigation, Formal analysis, Writing – original draft. **B. Campanella:** Writing – review & editing, Visualization. **V. Palleschi:** Writing – review & editing, Visualization. **M. Hidalgo:** Resources, Supervision, Writing – review & editing, Visualization. **S. Legnaioli:** Resources, Conceptualization, Project administration, Supervision, Writing – review & editing, Visualization.

## Declaration of Competing Interest

The authors declare that they have no known competing financial interests or personal relationships that could have appeared to influence the work reported in this paper.

## References

- [1] A. Miziolek, V. Palleschi, I. Schechter, *Laser Induced Breakdown Spectroscopy (LIBS): Fundamentals and Applications*, Cambridge University Press, Cambridge, 2006.
- [2] S. Musazzi, U. Perini, *Laser-Induced Breakdown Spectroscopy: Theory and Applications*, Springer, 2014.
- [3] Y. Li, D. Tian, Y. Ding, G. Yang, K. Liu, C. Wang, X. Han, A review of laser-induced breakdown spectroscopy signal enhancement, *Appl. Spectrosc. Rev.* 53 (1) (2018) 1–35.
- [4] D.A. Cremers, J.L. Radziemski, *Handbook of Laser Induced Breakdown Spectroscopy*, John Wiley & Sons, West Sussex, 2006.
- [5] N. Aras, S. Yalcin, Development and validation of a laser-induced breakdown spectroscopic method for ultra-trace determination of Cu, Mn, Cd and Pb metals in aqueous droplets after drying, *Talanta* 149 (2016) 53–61.
- [6] S. Niu, L. Zheng, A.Q. Khan, G. Feng, H. Zeng, Laser induced breakdown spectroscopic detection of trace level heavy metal in solution on a laser pretreated metallic target, *Talanta* 179 (2018) 312–317.
- [7] L. Fang, N. Zhao, M. Ma, D. Meng, Y. Jia, X. Huang, W. Liu, J. Liu, Detection of heavy metals in water samples by laser induced breakdown spectroscopy combined with annular groove graphite flakes, *Plasma Sci. Technol.* 21 (2018).
- [8] L. Ripoll, M. Hidalgo, Electrospray deposition followed by laser induced breakdown spectroscopy (EDS-LIBS): a new method for trace elemental analysis of aqueous samples, *J. Anal. At. Spectrom.* 34 (2019) 2016–2026.
- [9] S. Ma, Y. Tang, Y. Ma, Y. Chu, F. Chen, Z. Hu, Z. Zhu, L. Guo, X. Zeng, Y. Lu, Determination of trace heavy metal elements in aqueous solution using surface-enhanced laser-induced breakdown spectroscopy, *Opt. Express* 27 (10) (2019) 15091–15099.
- [10] M.A. Aguirre, S. Legnaioli, F. Almodovar, M. Hidalgo, V. Palleschi, A. Canals, Elemental analysis by surface-enhanced laser-induced breakdown spectroscopy combined with liquid-liquid microextraction, *Spectrochim. Acta Part B At. Spectrosc.* 279–80 (2013) 88–93.
- [11] X. Wang, L. Shi, Q. Lin, X. Zhu, Y. Duan, Simultaneous and sensitive analysis of Ag(I), Mn(II) and Cr(III) in aqueous solutions by LIBS combined with dispersive solid phase micro-extraction using nano-graphite as an adsorbent, *J. Anal. At. Spectrom.* 29 (2014) 1098–1104.
- [12] F.J. Ruiz, L. Ripoll, M. Hidalgo, A. Canals, Dispersive micro solid-phase extraction (D $\mu$ SPE) with graphene oxide as adsorbent for sensitive elemental analysis of aqueous samples by laser induced breakdown spectroscopy (LIBS), *Talanta* 191 (2019) 162–170.
- [13] L. Ripoll, J. Navarro-Gonzalez, S. Legnaioli, V. Palleschi, M. Hidalgo, Evaluation of thin film microextraction for trace elemental analysis of liquid samples using LIBS detection, *Talanta* 223 (2021).
- [14] L. Ripoll, S. Legnaioli, V. Palleschi, M. Hidalgo, Evaluation of electrosprayed graphene oxide coatings for elemental analysis by thin film microextraction followed by laser induced breakdown spectroscopy detection, *Spectrochim. Acta B At. Spectrosc.* 183 (2021).
- [15] A. De Giacomo, R. Gaudioso, C. Koral, M. Dell'Aglio, O. De Pascale, Nanoparticle-enhanced laser-induced breakdown spectroscopy of metallic samples, *Spectrochim. Acta B At. Spectrosc.* 85 (21) (2013) 10180–10187.
- [16] M. Dell'Aglio, R. Alrifai, A. De Giacomo, Nanoparticle enhanced laser induced breakdown spectroscopy (NELIBS), a first review, *Spectrochim. Acta Part B At. Spectrosc.* 148 (2018) 105–112.
- [17] A. De Giacomo, C. Koral, G. Valenza, R. Gaudioso, M. Dell'Aglio, Nanoparticle enhanced laser-induced breakdown spectroscopy for microdrop analysis at subppm level, *Anal. Chem.* 88 (10) (2016) 5251–5257.
- [18] X. Wen, Q. Lin, G. Liu, Q. Shi, X. Duan, Emission enhancement of laser-induced breakdown spectroscopy for aqueous sample analysis based on Au nanoparticles and solid-phase substrate, *Appl. Opt.* 55 (24) (2016) 6706–6712.
- [19] A. Pramanik, S. Karmakar, P. Kumbhakar, S. Biswas, R. Sarkar, P. Kumbhakar, Synthesis of bilayer graphene nanosheets by pulsed laser ablation in liquid and observation of its tunable nonlinearity, *Appl. Surf. Sci.* 449 (2020).
- [20] A. Botto, B. Campanella, I. Degano, S. Legnaioli, G. Lorenzetti, S. Pagnotta, F. Poggialini, V. Palleschi, Direct analysis of anthraquinone dyed textiles by surface enhanced Raman spectroscopy and Ag nanoparticles obtained by pulsed laser ablation, *Eur. Phys. J. Plus* 134 (2019) 414.
- [21] D. Paramelle, A. Sadovoy, S. Gorelik, P. Free, J. Hobbly, D.G. Fernig, A rapid method to estimate the concentration of citrate capped silver nanoparticles from UV-visible light spectra, *Analyst* 139 (2014) 4855–4861.
- [22] V.N. Popov, 2D Raman band of single-layer and bilayer graphene, *J. Phys. Conf. Ser.* 682 (2016).
- [23] L.M. Malard, M.A. Pimenta, G. Dresselhaus, M.S. Dresselhaus, Raman spectroscopy in graphene, *Phys. Rep.* 473 (2009) 51–87.
- [24] I. Duru, D. Ege, A.R. Kamali, Graphene oxides for removal of heavy and precious metals from wastewater, *J. Mater. Sci.* 51 (13) (2016) 6097–6116.
- [25] F. Perreault, A.F. De Faria, M. Elimelech, Environmental applications of graphene-based nanomaterials, *Chem. Soc. Rev.* 44 (16) (2015) 5861–5896.
- [26] R. Sitko, E. Turek, B. Zawisza, E. Malicka, E. Talik, J. Heimann, A. Gagor, B. Feist, R. Wrzalik, Adsorption of divalent metal ions from aqueous solutions using graphene oxide, *Dalton Trans.* 42 (2013) 5682–5689.
- [27] G. Zhao, J. Li, X. Ren, C. Chen, X. Wang, Few-layered graphene oxide Nanosheets as superior sorbents for heavy metal ion pollution management, *Environ. Sci. Technol.* 45 (24) (2011) 10454–10462.
- [28] W. Peng, H. Li, Y. Liu, S. Song, A review on heavy metal ions adsorption from water by graphene oxide and its composites, *J. Mol. Liq.* 230 (2017) 496–504.
- [29] G. Zhao, X. Ren, X. Gao, X. Tan, J. Li, C. Chen, Y. Huang, X. Wang, Removal of Pb(II) ions from aqueous solutions on few-layered graphene oxide nanosheets, *Dalton Trans.* 40 (2011) 10945–10952.
- [30] M. Kosmulski, The pH dependent surface charging and points of zero charge. IX. Update, *Adv. Colloid Interf. Sci.* 296 (2021), 102519.
- [31] R. Joyce, B.C. McKusick, *Handbook of Chemistry and Physics On-line: pH Range for Precipitation of Metal Hydroxides and Oxides*, Taylor and Francis Group, 2021 [Online]. Available: [https://hbcpc.chemetbase.com/faces/documents/08\\_69/08\\_69\\_0001.xhtml](https://hbcpc.chemetbase.com/faces/documents/08_69/08_69_0001.xhtml) [Consultato il giorno 26 05 2022].
- [32] M. Xia, C. Ye, K. Pi, D. Liu, A.R. Gerson, Cr(III) removal from simulated solution using hydrous magnesium oxide coated fly ash: optimization by response surface methodology (RSM), *Chin. J. Chem. Eng.* 26 (2018) 1192–1199.
- [33] A. Bertolini, G. Carelli, F. Francesconi, M. Francesconi, L. Marchesini, P. Marsili, F. Sorrentino, G. Cristoforetti, S. Legnaioli, V. Palleschi, L. Pardini, A. Salvetti, Modi: a new mobile instrument for in situ double-pulse LIBS analysis, *Anal. Bioanal. Chem.* 385 (2006) 240–247.
- [34] J. Pawliszyn, *Handbook of Solid Phase Microextraction*, Elsevier, 2012.